

Sulfonate-based networks between eukaryotic phytoplankton and heterotrophic bacteria in the surface ocean

Bryndan P. Durham¹*, Angela K. Boysen¹, Laura T. Carlson, Ryan D. Groussman, Katherine R. Heal, Kelsy R. Cain¹, Rhonda L. Morales, Sacha N. Coesel, Robert M. Morris, Anitra E. Ingalls and E. Virginia Armbrust

In the surface ocean, phytoplankton transform inorganic substrates into organic matter that fuels the activity of heterotrophic microorganisms, creating intricate metabolic networks that determine the extent of carbon recycling and storage in the ocean. Yet, the diversity of organic molecules and interacting organisms has hindered detection of specific relationships that mediate this large flux of energy and matter. Here, we show that a tightly coupled microbial network based on organic sulfur compounds (sulfonates) exists among key lineages of eukaryotic phytoplankton producers and heterotrophic bacterial consumers in the North Pacific Subtropical Gyre. We find that cultured eukaryotic phytoplankton taxa produce sulfonates, often at millimolar internal concentrations. These same phytoplankton-derived sulfonates support growth requirements of an open-ocean isolate of the SAR11 clade, the most abundant group of marine heterotrophic bacteria. Expression of putative sulfonate biosynthesis genes and sulfonate abundances in natural plankton communities over the diel cycle link sulfonate production to light availability. Contemporaneous expression of sulfonate catabolism genes in heterotrophic bacteria highlights active cycling of sulfonates in situ. Our study provides evidence that sulfonates serve as an ecologically important currency for nutrient and energy exchange between microbial autotrophs and heterotrophs, highlighting the importance of organic sulfur compounds in regulating ecosystem function.

Each year, marine phytoplankton generate nearly as much organic carbon as land plants¹. About half of this phytoplankton-produced organic matter is consumed by heterotrophic bacteria within minutes to weeks. This process constitutes the largest flux of organic carbon in the world's oceans and regulates the balance between remineralization to CO₂ and carbon storage². Organic compounds produced by phytoplankton differ in their elemental composition, redox state and biological availability, and bacteria have evolved diverse strategies for accessing and metabolizing these varied substrates. Organosulfur-based metabolisms exemplify the microbial networks that develop around the tight coupling of production and consumption of specific compounds. Phytoplankton leverage millimolar concentrations of sulfate in seawater to synthesize organic sulfur compounds with varying sulfur redox states (−2 to +6)³ that support a substantial portion of heterotrophic bacterial carbon, sulfur and energy needs⁴. The marine bacterial clades SAR11 and SAR86 fulfil sulfur requirements through exclusive use of organosulfur substrates with the most reduced form of sulfur (−2)^{5,6}, whereas the *Roseobacter* group preferentially uses substrates with reduced sulfur across a range of oxidation states (−2 to +4) despite their ability to reduce sulfate (+6)⁷. Whether an organosulfur compound fulfils heterotrophic sulfur requirements depends on the sulfur oxidation state and the bacterial lineage, with many compounds also able to fulfil carbon and energy requirements. Sulfonates are organosulfur compounds defined by their direct carbon–sulfur bond (R–SO₃[−]) in which the sulfur is in the +4/+5 oxidation state. Sulfonates are abundant in aerobic soils⁸ and terrestrial bacterial genomes harbour experimentally verified sulfonate transport and catabolism genes^{9–13}, suggesting their importance in

terrestrial ecosystems¹⁴. Many marine bacteria harbour homologues to terrestrial sulfonate transport and catabolism genes^{13,15–17}, and laboratory studies document the exchange of sulfonates between marine bacteria and eukaryotic phytoplankton^{18–22}. In particular, 2,3-dihydroxypropane-1-sulfonate (DHPS) is a major component of the diatom cytosol (~3 mM) that supports bacterial growth^{13,19} and is abundant in marine environments¹⁹, implicating sulfonates in trophic interactions in marine ecosystems. Efforts to examine the roles of sulfonates in situ are hampered by the fact that sulfonate biosynthesis routes and taxonomic sources are not well constrained in phytoplankton^{19,23,24}. Here, we combine laboratory studies with meta-transcriptomic and meta-metabolomic field analyses to disentangle sulfur-based phytoplankton–bacteria networks in the open ocean by mapping the flow of sulfonates through proposed phytoplankton biosynthetic and bacterial degradative pathways. Our results indicate that sulfonates are cycled along taxon-specific routes among major eukaryotic phytoplankton and heterotrophic bacterial lineages, revealing a prevalent metabolic link that mediates the tight coupling of organic matter production and consumption.

Results

As a first step in resolving taxonomic sources and biosynthetic pathways of C₂-sulfonates and C₃-sulfonates, we used metabolomics to screen intracellular metabolite pools of 36 plankton taxa, including autotrophic eukaryotic diatoms, dinoflagellates, haptophytes and prasinophytes, and autotrophic and heterotrophic bacteria (Table 1 and Supplementary Table 1). The C₃-sulfonates DHPS, sulfolactate and cysteate, and the C₂-sulfonates taurine and isethionate were measured quantitatively in cells (Supplementary Table 2).

School of Oceanography, University of Washington, Seattle, WA, USA. *e-mail: bpdurham@uw.edu

Table 1 | Sulfonates in various plankton monocultures

		DHPS ^a mM; amol cell ⁻¹	cysteate ^a μM; amol cell ⁻¹	sulfolactate ^a μM; amol cell ⁻¹	isethionate ^a mM; amol cell ⁻¹	taurine ^a mM; amol cell ⁻¹	DMSP ^b
Coccolithophores (haptophytes)							
<i>Emiliania huxleyi</i>	2090	9 ; 341	72 ; 3	-	-	0.08 ; 3	+
<i>E. huxleyi</i>	371	18 ; 715	43 ; 2	-	-	0.05 ; 2	+
Diatoms (stramenopiles)							
<i>C. meneghiniana</i>	338	15 ; 2,146	707 ; 99	3 ; <1	4 ; 621	0.04 ; 6	+
<i>Navicula pelliculosa</i>	543	7 ; 339	3 ; <1	1 ; <1	-	-	-
<i>Phaeodactylum tricornutum</i>	2561	5 ; 1,906	0.15 ; <1	0.04 ; <1	-	-	+
<i>P. pungens</i>	Pc55x	0.06 ; 92	5 ; 9	7 ; 12	20 ; 31,299	2 ; 2,822	+
<i>Thalassiosira oceanica</i>	1005	10 ; 1,455	0.65 ; <1	5 ; <1	-	-	+
<i>T. pseudonana</i>	1335	7 ; 433	0.85 ; <1	-	-	-	+
Dinoflagellates (alveolates)							
<i>Alexandrium tamarense</i>	1771	-	-	-	-	0.39 ; 6,705	+
<i>Amphidinium carterae</i>	1314	-	-	-	-	2 ; 1,210	+
<i>Heterocapsa triquetra</i>	449	-	-	-	-	0.38 ; 761	+
<i>Lingulodinium polyedra</i>	2021	-	-	-	-	0.56 ; 11,428	+
Prasinophytes (green algae)							
<i>M. pusilla</i>	1545	-	-	-	2 ; 8	4 ; 18	+
<i>Ostreococcus lucimarinus</i>	3430	-	161 ; <1	-	-	38 ; 38	+
Cyanobacteria							
<i>Crocospaera watsonii</i>	8501	-	8 ; <1	8 ; <1	-	-	-
<i>Prochlorococcus marinus</i>	1314x	-	37 ; <1	-	-	-	-
<i>P. marinus</i>	AS9601	-	28 ; <1	-	-	-	-
<i>P. marinus</i>	MED4	-	63 ; <1	-	-	-	-
<i>P. marinus</i>	NATL2A	-	219 ; <1	-	-	-	-
<i>Synechococcus</i> sp.	7803	-	67 ; <1	-	-	-	-
<i>Synechococcus</i> sp.	8102	-	-	-	-	-	-
Heterotrophic bacteria^d							
<i>Croceibacter</i> sp. (CFB)	SA60	-	2	<1	-	<1	-
<i>Hyphomonas</i> sp. (α)	SA36	-	<1	-	-	-	-
<i>Limnobacter</i> sp. (β)	SA59	-	<1	-	-	-	-
<i>Marinobacter</i> sp. (γ)	SA55	-	<1	-	-	-	-
<i>Pseudoalteromonas</i> sp. (γ)	SA7	-	<1	-	-	-	-
<i>Roseobacter denitrificans</i> (α)	Och 114	-	<1	-	-	-	-
<i>Roseovarius</i> sp. (α)	SA33	-	<1	-	-	<1	-
<i>Ruegeria pomeroyi</i> (α)	DSS-3	-	<1	-	-	<1	-
<i>Sulfitobacter</i> sp. (α)	SA11	-	<1	-	-	<1	+
<i>Sulfitobacter</i> sp. (α)	SA16	-	<1	-	-	<1	+
<i>Sulfitobacter</i> sp. (α)	SA30	-	<1	-	-	<1	+
<i>Sulfitobacter</i> sp. (α)	SA44	-	<1	-	-	<1	+
<i>Sulfitobacter</i> sp. (α)	SA48	-	<1	-	-	<1	-
<i>Sulfitobacter</i> sp. (α)	SA53	-	<1	-	-	<1	-
<i>Thalassospira</i> sp. (α)	SA42	-	<1	-	-	-	+

+, detected but not quantified; -, not detected. ^aEstimated cytosolic concentrations (indicated in bold) are based on phytoplankton cell volume and average attomoles of sulfonate per cell (see Supplementary Table 2 for exact values and further details). Cytosolic concentrations are not reported for heterotrophic bacteria because cell volume was not measured. ^bDMSP is reported for reference. ^cEukaryotic phytoplankton lineage is given in parentheses. ^dHeterotrophic bacterial lineage is given in parentheses: α, Alphaproteobacteria; β, Betaproteobacteria; CFB, *Cytophaga-Flavobacterium-Bacteroides*; γ, Gammaproteobacteria.

The sulfonium dimethylsulfoniopropionate (DMSP) and the taurine analogues homotaurine, methyl taurine and *N*-acetyltaurine were measured qualitatively.

The cultured organisms displayed taxon-specific combinations of C₂-sulfonates and C₃-sulfonates (Table 1). Consistently high

millimolar (5–18 mM) cytosolic concentrations of DHPS were exclusively detected in the diatoms and haptophytes; only the diatom *Pseudo-nitzschia pungens* contained substantially lower micromolar concentrations. DHPS co-occurred with the structurally related cysteate, indicating potential conversion between the two

molecules. Given that most cyanobacteria and all heterotrophic bacteria contained micromolar concentrations of cysteate, which can be an oxidation product of cysteine, this molecule probably serves as a common intermediate in sulfonate metabolism^{9,17,25}. The two prasinophytes displayed the highest cytosolic concentrations (4–38 mM) of taurine and produced three taurine analogues (Supplementary Table 2). Millimolar concentrations of isethionate were detected in the diatoms *Cyclotella meneghiniana* (4 mM) and *P. pungens* (20 mM) and the prasinophyte *Micromonas pusilla* (2 mM), all of which also produced taurine, indicating possible conversion between the two chemical analogues (Table 1). Neither DHPS nor isethionate was detected in bacteria, suggesting that they may be specific to eukaryotes in the surface ocean.

The high cytosolic concentrations of DHPS and isethionate in select eukaryotic phytoplankton suggest that they may help to protect cells against osmotic stress, as previously shown for a subset of sulfonates^{23,26}. In support of this hypothesis, we found that the diatom *Thalassiosira pseudonana* decreased intracellular DHPS concentrations by ~20-fold when grown under decreased salinity (35 versus 10 ppt; $P < 0.05$) (Supplementary Table 3). Other abundant compounds in *T. pseudonana*¹⁹ with osmoprotection roles—that is, DMSP, betaine, choline, glutamic acid and proline—decreased by ~5-fold to >100-fold under the same conditions. We estimate that DHPS accounts for ~3% of the cellular sulfur pool in *T. pseudonana* based on cellular stoichiometry²⁷, whereas the osmolyte DMSP¹⁹ and the sulfolipid sulfoquinovosyl diacylglycerol²⁸ account for ~4% and ~9% of the sulfur pool, respectively.

To infer eukaryotic phytoplankton biosynthetic pathways for C₂-sulfonates and C₃-sulfonates informed by the metabolite data, we searched publicly available eukaryotic genomic and transcriptomic data to identify homologues to experimentally verified genes involved in sulfonate metabolism in heterotrophic bacteria, archaea and/or multicellular eukaryotes (Fig. 1 and Supplementary Table 4). An underlying assumption in this gene homology search was that known reversible enzymes in prokaryotes could potentially catalyse reversible reactions in eukaryotes; specifically, forward and reverse reactions have been experimentally demonstrated in vitro for sulfolactate dehydrogenase (encoded by *comC*) and cysteate aminotransferase (encoded by *CoA*) enzymes described herein^{12,29} (Fig. 1). Putative eukaryotic homologues were required to be reciprocal best hits to experimentally verified proteins (Supplementary Table 4) and/or to cluster with experimentally verified proteins on a maximum-likelihood phylogenetic tree (Supplementary Fig. 1). All major eukaryotic phytoplankton lineages possess homologues to the serine dehydratase (*SDH*) gene that is required to convert serine into aminoacrylate, a precursor to both pyruvate, for gluconeogenesis, and cysteate, for C₂-sulfonate and C₃-sulfonate metabolism³⁰ (Fig. 1). No *SDH* homologues were detected in cyanobacteria, which presumably harbour an alternative pathway to produce cysteate. The C₂-sulfonate taurine can be derived from cysteate through a decarboxylation step or, alternatively, taurine can be produced from cysteine via the cysteine dioxygenase (*CDO1*) and cysteine sulfinic acid decarboxylase (*CSAD*) genes^{30,31}. A subset of cyanobacteria and eukaryotic phytoplankton possess *CDO1* homologues (Fig. 1 and Supplementary Table 4), indicating that both the serine-derived and the cysteine-derived pathways are used for taurine biosynthesis in eukaryotic phytoplankton. However, *SDH* gene homologues are more prevalent in certain taxa³⁰. For example, while a small number of green algae (for example, *Chlamydomonas* and *Chloroparvula*) harbour *CDO1* homologues, the two prasinophytes that contained high cytosolic concentrations (4–38 mM) of taurine (Table 1) only harbour *SDH* homologues for the serine-derived pathway (Supplementary Table 4). Production of isethionate has been characterized only in a bacterial catabolic pathway as a waste product during taurine catabolism³². The presence of both isethionate and its chemical analogue taurine in a subset of prasinophytes and diatoms

(Table 1) suggests that isethionate is formed from taurine through a homologous eukaryotic pathway (Fig. 1). The first step in converting taurine to isethionate is carried out by taurine aminotransferase (encoded by *tpa/toa*). Gene homologues for *tpa/toa* were found in all phytoplankton genomes (Fig. 1 and Supplementary Table 4); however, we note that these enzymes belong to a large aminotransferase protein family that acts on various substrates. The second step is carried out by sulfoacetaldehyde reductase (encoded by *isfD*). Homologues to this gene were identified in prasinophytes, but not in diatoms (Supplementary Table 4), despite the fact that two diatoms contained high concentrations of isethionate (Table 1). This enzyme belongs to a diverse family of short-chain dehydrogenases/reductases; in diatoms, the reaction may be carried out by a related, but uncharacterized, reductase. Haptophytes and dinoflagellates also possess *isfD* homologues (Supplementary Table 4), although measurable levels of isethionate were not detected, suggesting that either its production is conditional or the pathway is not functional.

C₃-sulfonates are found in the metabolisms of several marine and terrestrial taxa. The C₃-sulfonates sulfolactate and DHPS can be generated through the degradation of sulfoquinovose (6-deoxy-6-sulfolglucose) in terrestrial bacteria^{11,33}. A complete set of gene homologues for these pathways was not detected in phytoplankton genomes nor was the sulfolactaldehyde intermediate common to these pathways present in our culture metabolomes. Instead, we hypothesize that eukaryotic phytoplankton convert C₃-sulfonate precursor cysteate to sulfolactate via *CoA* and *comC* genes (Fig. 1), which are used by methanogenic archaea during biosynthesis of coenzyme M (2-mercaptoethanesulfonate) and by heterotrophic bacteria during sulfonate catabolism^{16,25}. Homologues for both *CoA* and *comC* were detected in diatoms, haptophytes and dinoflagellates based on sequence similarity and phylogenetic clustering with experimentally verified sequences (Supplementary Fig. 1 and Supplementary Table 4). The structural similarity of DHPS to both sulfolactate and the glycolysis intermediate glycerol phosphate led us to evaluate whether DHPS could be synthesized by reactions similar to those used in cysteate–sulfolactate transformation or through a phosphate–sulfonate moiety transfer, respectively (Fig. 1). Previous ³⁵S-radiolabelling experiments in diatoms suggested that DHPS was produced by reductive deamination of cysteinolic acid³⁴. We identified a mass spectral feature within the untargeted metabolomes of the cultures with the exact mass of cysteinolic acid ($m/z = 156.0321$) and an isotopic signature that requires inclusion of sulfur in its molecular formula (C₅H₉NO₄S) (Supplementary Fig. 2). While the lack of a commercially available standard precludes confirmation of its identity, the mass spectral fragmentation pattern is consistent with the structure of cysteinolic acid, and our culture observations are consistent with previous measurements of cysteinolic acid in marine phytoplankton that used an authentic standard^{34,35}. The putative cysteinolic acid was detected in all diatom and haptophyte cultures in which DHPS was detected, in addition to a subset of dinoflagellates and heterotrophic bacteria that do not produce DHPS (Supplementary Table 2). We hypothesize that *CoA* and *comC* homologues in select eukaryotic phytoplankton allow them to carry out transformations of cysteinolic acid and DHPS in a manner homologous to cysteate–sulfolactate transformations. Indeed, these enzymes are known to be promiscuous and act on structurally similar substrates^{29,36}. Together, these data support the proposed cysteate-derived pathway rather than an alternate pathway in which DHPS is produced from glycerol phosphate (Fig. 1).

Identification of gene homologues in the putative sulfonate biosynthetic pathways allowed us to expand our analyses beyond cultured phytoplankton isolates and interrogate eukaryotic metatranscriptomes to explore the potential pervasiveness of sulfonate cycling in natural open-ocean communities. We examined transcriptional profiles over the diel cycle because sulfate assimilation in plants is tightly coupled to day–night rhythms³⁷, with the

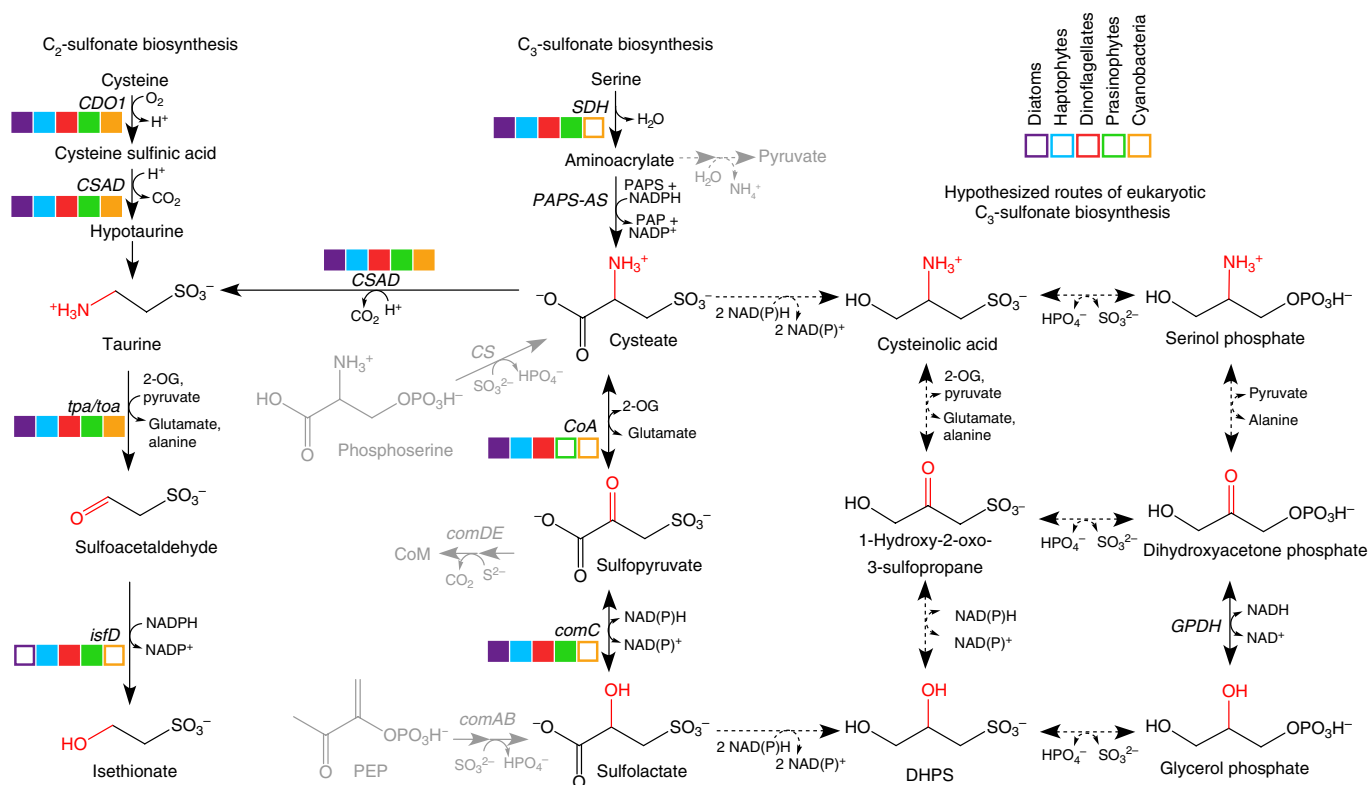


Fig. 1 | Predicted C_2 -sulfonate and C_3 -sulfonate biosynthesis routes in eukaryotic phytoplankton. Left, C_2 -sulfonate biosynthesis begins with the conversion of cysteine or cysteate into taurine via the *CDO1* and *CSAD* genes^{30,31} followed by the transformation of taurine to isethionate via the *tpa/toa* and *isfD* genes experimentally verified in heterotrophic bacteria³². Middle, C_3 -sulfonate biosynthesis begins with the conversion of serine to cysteate via the *SDH* and 3'-phosphoadenylyl sulfate:2-aminoacrylate C-sulfotransferase (*PAPS-AS*) genes described in algae³⁰ followed by transformation of cysteate to sulfolactate via the *CoA* and *comC* genes experimentally verified in heterotrophic bacteria and archaea^{2,29}. Additional reactions including the spontaneous production of pyruvate from aminoacrylate and those involved in archaeal biosynthesis of C_2 -sulfonate coenzyme M (CoM) are in grey. The presence of gene homologues in marine phytoplankton lineages (identified in genomes (Supplementary Table 4) and eukaryotic transcriptome assemblies) are indicated with the filled coloured boxes. Right, hypothesized biosynthetic pathways of C_3 -sulfonates cysteinolic acid and DHPS in eukaryotic phytoplankton are shown with dashed arrows. Cysteinolic acid and DHPS may be produced by the reduction of cysteate and sulfolactate, respectively, or the sulfonation of dihydroxyacetone phosphate and/or its derivatives serinol phosphate and glycerol phosphate. Conversion between DHPS and cysteinolic acid probably occurs through *CoA* and *comC* homologues. Amino and hydroxyl groups and their carbonyl intermediates are coloured in red. 2-OG, 2-oxoglutarate; *GPDH*, glycerol-3-phosphate dehydrogenase; PAPS, 3'-phosphoadenosine-5'-phosphosulfate; PEP, phosphoenolpyruvic acid.

expectation that sulfonate biosynthesis would similarly reflect daily phytoplankton activity. RNA samples were collected for eukaryotic metatranscriptomes every 4 h over the course of 4 d from a surface water parcel in the North Pacific Subtropical Gyre. We also analysed publicly available prokaryotic metatranscriptomes derived from the same diel study³⁸ to assess bacterial gene expression patterns.

Taxon-specific transcriptional patterns were quantitatively determined for genes required for sulfate assimilation and for gene homologues that we predict are involved in sulfonate biosynthesis (Fig. 1 and Supplementary Table 5). Transcripts for the sulfate assimilation genes encoding sulfate adenylyltransferase (*APS*, *cysD*), (phospho)adenosine 5'-phosphosulfate reductase (*APR*, *cysH*) and sulfite reductase (*SIR*, *sir*) were detected for all major eukaryotic phytoplankton and cyanobacteria groups (Fig. 2a and Supplementary Fig. 3). Many of these transcripts exhibited diel periodicity in abundance, consistent with sulfate being an essential macronutrient tied directly to marine primary productivity³⁹. We also detected transcripts for the putative sulfonate biosynthesis homologues *CDO1*, *CSAD* and *isfD* (C_2 -sulfonate biosynthesis) and *SDH*, *CoA* and *comC* (C_3 -sulfonate biosynthesis) (Fig. 2a), allowing us to examine which organisms may be producing sulfonates in the environment. The taxonomy of the open-ocean transcripts matched our expectations from the laboratory studies; transcripts for the full set of putative

sulfonate gene homologues were detected in haptophytes and stramenopiles while no *CoA* transcripts were detected in green algae. Haptophytes and stramenopiles displayed the most striking diel expression patterns in sulfate assimilation transcripts. Recurring daily peaks in transcript abundance for *APS* and *APR* occurred near dawn, and near dusk for *SIR* (Fig. 2b), consistent with transcription of plant *APS* and *APR* being a key regulatory step in light-regulated sulfate assimilation. The putative C_2 -sulfonate biosynthesis gene *CDO1* was transcribed by all eukaryotic taxa over the diel cycle, with the exception of green algae, which do not typically harbour this gene³⁰ (Fig. 2a and Supplementary Table 4). Only haptophytes displayed significant diel periodicity in *CDO1* transcript abundance. The putative C_3 -sulfonate biosynthesis gene *SDH* displayed periodic transcript abundances in haptophytes, but not in stramenopiles, whereas transcripts for the putative *CoA* gene showed diel periodicity in stramenopiles, but not haptophytes. These transcriptional patterns indicate that the first steps of C_2 -sulfonate and C_3 -sulfonate biosynthesis (*CDO1* and *SDH*) may be important regulatory points in haptophytes, with differences in transcriptional timing possibly reflecting substrate availability over the diel cycle. Sequences related to the haptophyte genus *Chrysochromulina* stood out in our phylogenetic analysis of the diel oscillating sulfonate biosynthesis transcripts. Thus, we obtained laboratory cultures of *Chrysochromulina acantha*,

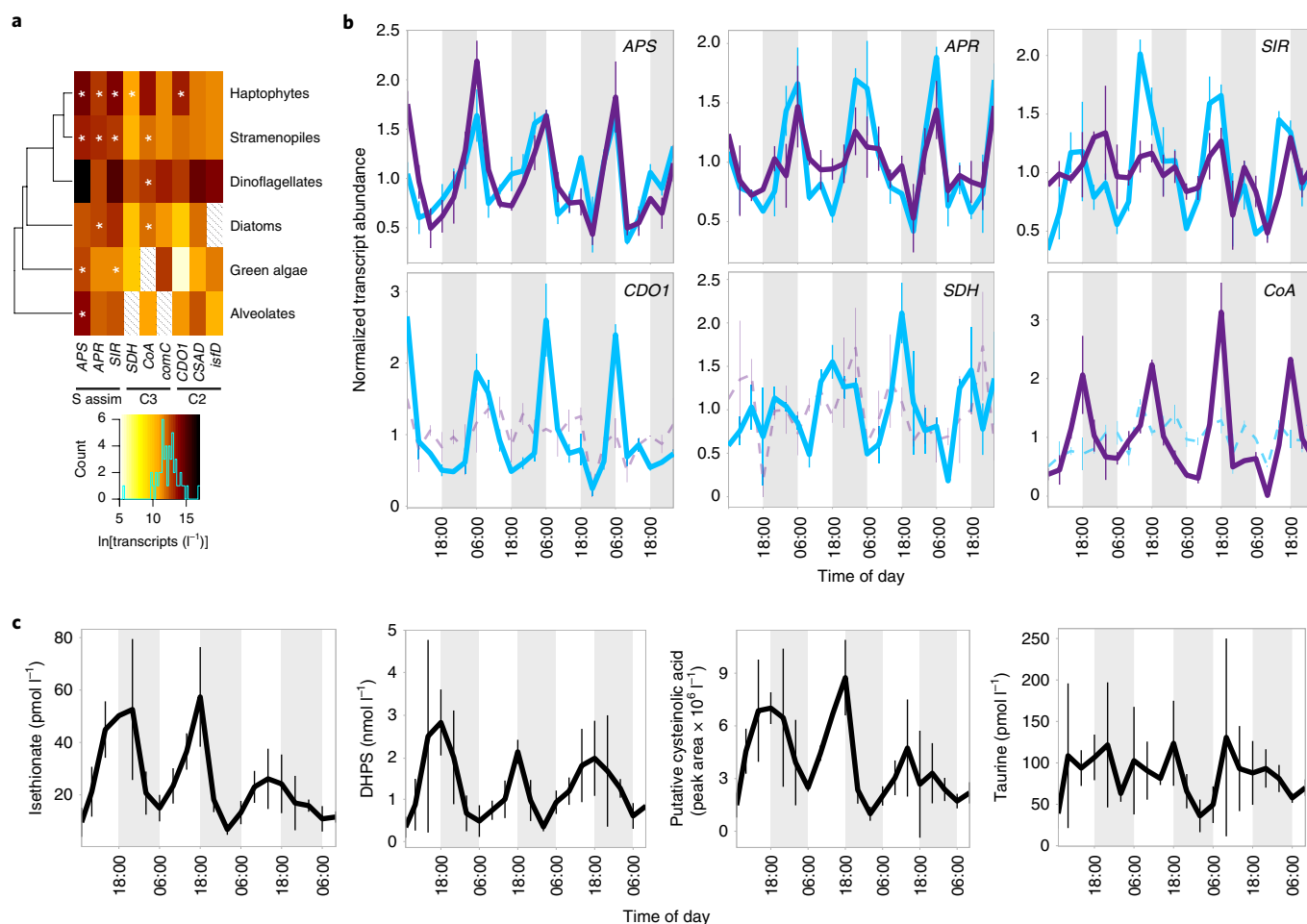


Fig. 2 | Daily sulfonate dynamics over a 4-d period in the North Pacific Subtropical Gyre. a, In mean transcript abundances per litre of seawater over 4 d ($n=48$) for sulfate assimilation (S assim) and sulfonate biosynthesis (C_2 and C_3) gene homologues in major eukaryotic phytoplankton taxa. The asterisks denote those genes with statistically significant diel periodicity based on the RAIN package⁶⁹ with the false discovery rate Bonferroni correction method ($P < 0.05$). The dotted lines indicate that the gene homologue is not present in the taxon. Diatoms and dinoflagellates were analysed separately and thus are not included in the denoted stramenopile and alveolate groups. The legend shows the \ln transcript abundance colour code and gene counts by transcript abundance bin. **b**, Mean transcript abundance of sulfate assimilation and sulfonate metabolism gene homologues in haptophytes (blue) and stramenopiles (purple) per time point ($n=2$) versus transcript mean over the course of the diel study ($n=48$). Those transcripts that showed statistically significant periodicity are in bold; those transcripts that were not significant are shown with dashed lines. The error bars represent the range of biological duplicates ($n=2$). **c**, Mean sulfonate abundances in North Pacific Subtropical Gyre plankton that showed statistically significant diel periodicity based on the RAIN package⁶⁹ with the false discovery rate Bonferroni correction method ($P < 0.05$) over the course of the diel study. The error bars represent the standard deviation of biological triplicates ($n=3$).

Chrysochromulina rotalis and *Chrysochromulina simplex* and were able to detect appreciable amounts of DHPS, taurine and isethionate in all three cultures (Supplementary Table 6). This finding along with the corresponding presence of sulfonate gene homologues in publicly available *Chrysochromulina* transcriptomes provides confidence for our proposed biosynthetic pathways and indicates that their open-ocean relatives are probably important sulfonate producers in the gyre.

The diel periodicity of sulfate assimilation and putative sulfonate biosynthesis transcripts (Fig. 2b) suggests that sulfonate production in haptophytes and stramenopiles is regulated over the diel cycle in the North Pacific. We quantified five sulfonates (taurine, isethionate, DHPS, cysteate and sulfolactate) in particulate cellular material collected concurrently with the metatranscriptome samples (Supplementary Table 7). We note that these sulfonates represent a subset of uncharacterized organic sulfur compounds; we detected 19 additional sulfur-containing metabolites in the untargeted metabolite data with no match in publicly available MS² databases

(Supplementary Table 8). Isethionate and DHPS displayed significant ($P < 4 \times 10^{-8}$) diel rhythms in abundance, and the mass spectral feature putatively identified as cysteinolic acid also displayed significant ($P < 3 \times 10^{-7}$) periodicity (Fig. 2c and Supplementary Table 9). The abundance of taurine was also significantly ($P < 6 \times 10^{-4}$) diel, although the signal was dampened probably due to production by multiple autotrophic and heterotrophic organisms (Fig. 2c). Cysteate (median: 3 pmol l^{-1}) and sulfolactate (median: 6 pmol l^{-1}) did not vary significantly over the diel cycle perhaps due to their functions as intermediates in organosulfur metabolism across a broad spectrum of organisms (Supplementary Fig. 4). Mean abundances of DHPS (range: 339 ± 249 to $2,816 \pm 780 \text{ pmol l}^{-1}$) and isethionate (range: 7 ± 2 to $57 \pm 19 \text{ pmol l}^{-1}$) increased by 3–7-fold over the course of the day, and the putative cysteinolic acid increased by 3–5-fold (based on relative changes in peak area), with corresponding decreases over the course of the night. These diel oscillations are consistent with a role in maintaining redox balance during photoautotrophic metabolism. Sulfonates may have higher flux and

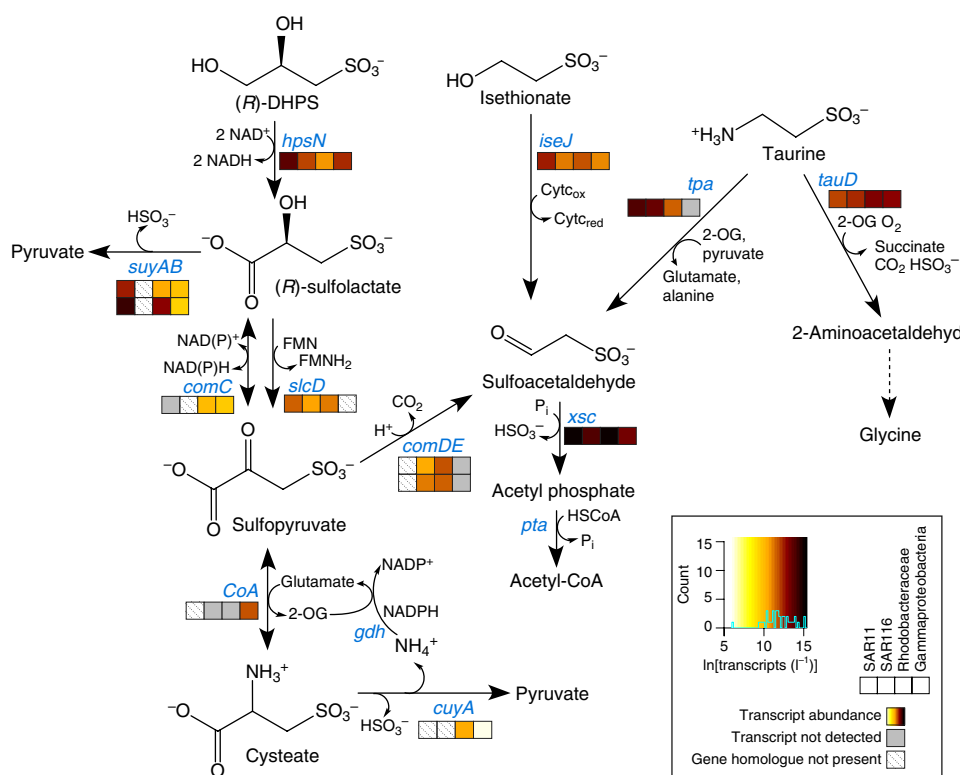


Fig. 3 | C_2 -sulfonate and C_3 -sulfonate catabolism by heterotrophic bacteria in the North Pacific Subtropical Gyre. Mean transcript inventories per litre of seawater ($n = 2$) for gene homologues (blue) in major heterotrophic prokaryotic taxa. The legend shows the \ln transcript abundance colour code and the gene counts by transcript abundance bin. Gene homologues that are present in the taxon but for which no transcripts were detected are shown in grey. Enzyme names for corresponding genes are as follows: *comDE*, sulfopyruvate decarboxylase; *gdh*, glutamate dehydrogenase; *hpsN*, DHPS 3-dehydrogenase; *iseJ*, isethionate dehydrogenase; *pta*, phosphate acetyltransferase; *slcD*, sulfolactate dehydrogenase; *suyAB*, sulfolactate sulfolyase; *tauD*, taurine dioxygenase; *cuyA*, L-cysteate sulfolyase. CoA, coenzyme A; Cyt_c, cytochrome c; FMN, flavin mononucleotide.

accumulate under conditions of excess reducing power, as occurs during the daytime, and decrease at night due to catabolism and/or excretion. Whether sulfonates are actively (via export) or passively (via cell lysis) released into the dissolved phase is unknown, in part because of analytical challenges with measuring these small, polar molecules extracellularly in seawater⁴⁰.

Gene expression analysis of bacterial catabolic pathways provides a useful tool for inferring the presence of low-abundance compounds rapidly cycled by heterotrophic bacteria⁴¹. To discern the flow of phytoplankton-produced sulfonates through heterotrophic bacterial communities, we quantitatively determined bacterial transcript inventories of lineage-specific degradation routes for individual sulfonates based on prokaryotic metatranscriptomes collected at dawn from surface water near our diel study (Fig. 3). Sulfonate catabolism transcripts were identified by homology to experimentally demonstrated and putative catabolic genes in members of the *Roseobacter* (within the Rhodobacteraceae), SAR11 and SAR116 lineages^{13,15–17} that together make up ~50% of the surface ocean bacterial community¹², as well as Vibrionales and Oceanospirillales lineages (Gammaproteobacteria)¹⁹ (Supplementary Table 10). A majority of transcripts associated with sulfonate catabolism belonged to the numerically dominant SAR11 clade ($\sim 8.1 \times 10^6$ transcripts l^{-1}). Sulfonate catabolism transcripts were detected at lower abundances for the Rhodobacteraceae ($\sim 5.2 \times 10^6$ transcripts l^{-1}), SAR116 ($\sim 2.5 \times 10^6$ transcripts l^{-1}) and Gammaproteobacteria ($\sim 1.5 \times 10^6$ transcripts l^{-1}) groups (Fig. 3). The highest transcript inventories involved in sulfonate catabolism were derived from the sulfoacetaldehyde acetyltransferase gene (*xsc*), probably reflecting the prevalence of this gene in marine bacteria (Supplementary Table 10)

as sulfoacetaldehyde is a common intermediate in C_2 -sulfonate and C_3 -sulfonate catabolism (Fig. 3). The second highest transcript abundances were involved in catabolism of taurine (*tpa*, *tauD*) followed by DHPS (*hpsN*) and isethionate (*iseJ*). Thus, these molecules are released from phytoplankton cells at high enough concentrations to trigger bacterial utilization.

The catabolic fates of different sulfonates were inferred from the bacterial metatranscriptomes. Taurine is catabolized in two ways: either to acetyl-CoA via a sulfoacetaldehyde intermediate or to 2-aminoacetaldehyde. Transcripts for genes involved in both transformations (*tpa* and *tauD*, respectively) were detected in the four major heterotrophic bacterial groups with the exception that no gammaproteobacterial *tpa* transcripts were detected. An alternate route for conversion of taurine to sulfoacetaldehyde is carried out by taurine dehydrogenase (encoded by *tauXY*), although few marine bacterial genomes harbour this pathway (Supplementary Table 10), and no transcripts were detected in our samples. Subsequent metabolism of 2-aminoacetaldehyde is unknown, although based on structural similarity, we hypothesize that it is oxidized to glycine (Fig. 3). Transcripts from all groups were detected for the isethionate catabolism gene *iseJ*, which encodes the enzyme involved in isethionate degradation to sulfoacetaldehyde for subsequent acetyl-CoA production (Fig. 3). While the SAR11 clade appears to primarily catabolize DHPS directly to pyruvate via sulfolactate (*hpsN* and *suyAB*), the SAR116, Rhodobacterales and Gammaproteobacteria groups harbour additional genes to generate acetyl-CoA via sulfoacetaldehyde (*comDE*) or pyruvate via cysteine (*cuyA*) (Fig. 3). Thus, these lineages have access to a larger suite of sulfonates; for instance, members of the *Roseobacter* group can directly transport

and catabolize the C₃-sulfonate intermediates sulfolactate and cysteate^{16,17}, which are present in phytoplankton cells at low concentrations (Table 1). Furthermore, the three desulfonation reactions (encoded by *suyAB*, *cuyA* and *xsc*) release sulfur in the form of bisulfite, which can be assimilated by *Roseobacter* members²². By contrast, bisulfite produced via desulfonation routes in the SAR11 clade (*suyAB* and *xsc*) is ultimately remineralized to sulfate.

Our metatranscriptomic analyses suggest that SAR11 consumes sulfonates in the open ocean. To test this, we used DHPS as a substrate to isolate an open-ocean SAR11 strain from the North Pacific. Strain NP1 was acclimated to defined artificial seawater media with methionine (−2 sulfur oxidation state) as the sulfur source, pyruvate as the carbon and energy source, and glycine to fulfil the known SAR11 auxotrophic requirement^{43,44}. Cells were subsequently acclimated to media in which methionine, pyruvate and glycine were replaced with equal molar amounts of DMSP (−2 sulfur oxidation state) as the sulfur source, DHPS as the carbon and energy source, and taurine as the precursor for glycine. Growth rates were not significantly different between the two treatments (Supplementary Tables 11 and 12). However, cultures reached significantly higher cell yields (~3-fold, $P < 0.01$) when grown on the fully organic sulfur-based media rather than the standard growth media (Supplementary Tables 11 and 12 and Supplementary Fig. 5), suggesting a higher growth efficiency with DHPS than with pyruvate. Regardless of which variations of growth media were tested, inclusion of DHPS as the carbon source always resulted in significantly higher cell yields (~3-fold, $P < 0.05$; Supplementary Table 12) than inclusion of pyruvate. We also found that strain NP1 can use taurine as a carbon source, as previously shown in SAR11 (refs. 43,44), and as a glycine substitute (Fig. 3). Growth on DMSP and taurine, with or without DHPS, resulted in similar growth rates and cell yields ($P > 0.05$; Supplementary Table 12). Together, these data demonstrate that both DHPS and taurine can substitute for pyruvate in SAR11, and that taurine can additionally act as a glycine substitute via a cryptic pathway that probably involves *tauD* and the production of 2-aminoacetaldehyde (Fig. 3). We note that single (DMSP) and double (DMSP and DHPS) substitutions in combination with glycine resulted in significantly slower growth rates (~2-fold, $P < 0.05$) than with either methionine–pyruvate–glycine or DMSP–DHPS–taurine (Supplementary Tables 11 and 12 and Supplementary Fig. 5). This reduction in growth rate may reflect glycine-dependent regulation of carbon metabolism for biosynthesis and energy in SAR11 (ref. 45) and/or potential toxicity associated with DMSP catabolism⁴⁶. Although DMSP can serve as a carbon source in addition to a source of reduced sulfur⁴⁷, there was no significant difference between cell yields when DMSP was substituted for methionine. These results, in combination with the observation that all publicly available SAR11 genomes from the surface ocean harbour genes encoding DHPS, taurine and isethionate degradation, indicate the importance of eukaryotic phytoplankton-derived sulfonates for SAR11 growth.

Discussion

Our study highlights how microorganisms partition their chemical environment to create guilds of coexisting producers and consumers, centred in this instance around specific organic sulfur compounds. We show that eukaryotic haptophytes and stramenopiles are major producers of the C₃-sulfonate DHPS. Biosynthesis of C₂-sulfonates seems to be phylogenetically widespread across eukaryotic phytoplankton lineages, although our metabolomic surveys suggest that isethionate production is more restricted. The ability to biosynthesize the C₃-sulfonates is constrained to those lineages that possess homologues to *CoA* and *comC* genes known from archaea and bacteria, suggesting that an early gene transfer event permitted haptophyte and stramenopile lineages to convert amino-containing sulfonates (cysteate and cysteinolic acid) to their

hydroxyl analogues (sulfolactate and DHPS). While sulfonates display characteristics of compatible solutes that accumulate to high internal concentrations within cells (>10 mM; Table 1), their full set of roles within organisms remains unclear. The strong diel oscillations in abundance of C₃-sulfonates (Fig. 2) and their striking resemblance to sulfolglycolysis intermediates^{11,33} (Fig. 1) suggests that this subset of sulfonates may be used in eukaryotic phytoplankton for redox balance and/or short-term storage and regeneration of intermediates in central metabolism.

Two major alphaproteobacterial lineages, *Roseobacter* and SAR11, illustrate the ecological partitioning of sulfonate catabolism (Fig. 3). *Roseobacter* members harbour larger genomes that often encode motility, chemotaxis and defence functions that enable direct interactions with phytoplankton cells⁴⁸. Genome expansion of the *Roseobacter* lineage coincided with the radiation of red-lineage phytoplankton ~260 million years ago⁴⁹, which may explain their large repertoire of regulatory and functional genes for sulfonate transport and catabolism. By contrast, SAR11 members are non-motile, planktonic cells with smaller genomes. This clade harbours pathways for degradation of the most abundant sulfonates, for example, DHPS, isethionate and taurine. No known sulfonate transcriptional regulators are present in SAR11 genomes, consistent with their limited regulatory capacity and evolution to scavenge readily available, low-molecular-weight substrates⁵⁰. Moreover, we show that three organosulfur compounds primarily derived from eukaryotes, DMSP and the sulfonates DHPS and taurine can fully support heterotrophic metabolism of open-ocean SAR11, demonstrating the importance of organosulfur-based heterotrophy in the oligotrophic ocean. The observed ubiquity and homology of sulfonate metabolism among marine and terrestrial microorganisms reveal the prevalence and essential role of sulfonate-based dependencies in structuring microbial networks.

Methods

Plankton culturing and collection. Heterotrophic bacteria were streaked to isolation on ½ YTSS agar at 25–30 °C in the dark for 2–5 d, after which isolated colonies were inoculated into artificial L1 seawater medium amended with carbon, nitrogen, amino acid and vitamin sources (see Supplementary Table 1 for details) and grown overnight at 30 °C in the dark at 200 r.p.m. in VWR SuperClear Ultra-High Performance conical tubes. Overnight cultures were diluted to ~0.01 optical density (OD) into fresh L1 medium and grown overnight until cells reached late exponential phase/early stationary phase (~0.2–0.4 OD). Cells were collected by gentle filtration onto 0.2-µm Durapore filters using combusted borosilicate filter towers, flash frozen in liquid nitrogen and subsequently stored at −80 °C until metabolite extraction.

Axenic phytoplankton were cultured in combusted borosilicate tubes in diurnal incubators under optimum medium, light and temperature conditions (see Supplementary Table 1 for details). Cells were collected at mid-light cycle during mid-to-late exponential phase by gentle filtration onto 0.2-µm Durapore filters using combusted borosilicate filter towers. All filters were flash frozen in liquid nitrogen and subsequently stored at −80 °C. The axenic status of phytoplankton was verified regularly using 4,6-diamidino-2-phenylindole staining and epifluorescence microscopy, SYBR staining and flow cytometry, along with plating on bacterial ½ YTSS agar. Three non-axenic cultures of *Chrysochromulina* (*C. acantha* K-0643, *C. rotalis* K-0644 and *C. simplex* K-0272) were cultured in natural seawater-based L1 medium at 15 °C on a 12 h/12 h light–dark cycle at ~50 µmol photons m^{−2} s^{−1}. Approximately 10⁷ cells were collected by centrifugation and frozen at −80 °C until metabolite extraction.

Culture metabolomics. Frozen filters of cells and media blanks were extracted for liquid chromatography–mass spectrometry-based metabolomics according to the protocol in Boysen and Heal et al.⁵¹ that yields two metabolite fractions, a non-polar organic fraction and a highly polar aqueous fraction. Sulfonates are recovered in the aqueous fraction. Targeted metabolomics data were generated using a Waters Xevo TQ-S triple quadrupole with both reversed-phase and hydrophilic interaction liquid chromatography (HILIC). Peaks were integrated using Skyline v4.1 for small molecules⁵². Untargeted metabolomics data were generated using a Thermo QExactive HF with HILIC. DHPS was provided by A. Bourdon and S. Champagna (University of Tennessee, Knoxville, TN, USA); *N*-acetyltaurine was provided by A. Cook and K. Denger (University of Konstanz, Konstanz, Germany); and DMSP was provided by W. Whitman and M. Moran (University of Georgia, Athens, Georgia, USA). All other sulfonate standards are available commercially.

Taurine, isethionate, sulfolactate and cysteate were quantified using isotopically labelled internal standards. DHPS was quantified by generating standard addition curves. Detailed information about standards is included in Boysen and Heal et al.⁵¹. Cytosolic concentrations were calculated based on cell volume values (Supplementary Table 2).

Field metabolomics. Plankton were collected during R/V Kilo Moana cruise KM1513 (July–August 2015) near Station ALOHA in the North Pacific Subtropical Gyre by following free-drifting drogues centred at a depth of 15 m. Triplicate plankton samples of ~3.5 l of surface seawater from a depth of 15 m were collected every 4 h over the course of 4 d (26–30 July 2015), yielding 72 samples in total. Plankton were filtered onto a 47-mm 0.2- μ m Omnipore filter using a peristaltic pump. Filters were flash frozen in liquid nitrogen and subsequently stored at -80°C until further processing. Metabolite extractions and metabolomics data analysis were carried out as described above, with detailed information in Boysen and Heal et al.⁵¹.

Untargeted metabolomics analyses. To identify metabolites that contain sulfur, a search algorithm was used to obtain mass spectral features that contain the natural isotope pattern of sulfur in the untargeted metabolomics data from the HILIC (processed using XCMS v3.7 in R⁵³). This search algorithm has been previously used and described for identifying iron-containing compounds⁵⁴. In short, candidate masses that contain sulfur were obtained by identifying features that have a mass and abundance ratio of ^{32}S (94.9%) and ^{34}S (4.2%). These peaks were visually inspected to ensure a high-quality peak in both isotopes at the expected ratio. Methodological blanks were also inspected to ensure that these peaks were not present in any appreciable amount (average sample peak areas must be at least three times the size of the methodological blanks). Compounds were removed from this list that were the ^{13}C or ^{15}N isotopes of other S-containing compounds. Publicly available MS² databases, that is Metlin or MassBank, were used for compound identification. Cysteinolic acid (previously described in phytoplankton by Busby and colleagues^{34,35}) was putatively identified by its mass to charge ($m/z = 156.0321$ in positive ionization mode) and sulfur search algorithm in a sample of *T. pseudonana*. MS² fragments were identified using MS-DIAL v3.08 (ref. ⁵⁵) and Thermo Scientific Xcaliber software v4.1, and molecular formulas were identified by their mass⁵⁶.

Metatranscriptomics. Eukaryotic metatranscriptome samples were collected during R/V Kilo Moana cruise KM1513 (July–August 2015) near Station ALOHA in the North Pacific Subtropical Gyre by following free-drifting drogues centred at a depth of 15 m. Duplicate plankton samples of ~7 l of seawater were collected from a depth of 15 m every 4 h over the course of 4 d, yielding 48 samples in total. Plankton were sequentially filtered through a 100- μ m nylon mesh pre-filter followed by a 142-mm 0.2- μ m polycarbonate filter using a peristaltic pump. Filters were flash frozen in liquid nitrogen and subsequently stored at -80°C until further processing. Filters were extracted using the ToTALLY RNA Kit (Invitrogen) with some modifications. Briefly, frozen filters were added to 50-ml falcon tubes containing 5 ml of denaturation solution and extraction beads (125 μ l of 100- μ m zirconia beads, 125 μ l of 500- μ m zirconia beads and 250 μ l of 425–600- μ m silica glass beads). In addition, to generate quantitative transcript inventories, a set of 14 internal mRNA standards were also added to the extraction buffer; these standards were synthesized as previously described⁵⁷, with the exception that eight standards were synthesized with poly(A) tails to mimic eukaryotic mRNAs. Total, extracted RNA was treated with DNase I (Ambion) and purified with DNase inactivation reagent (Ambion). Eukaryotic mRNAs were poly(A)-selected, sheared to ~225-bp fragments and used to construct TruSeq complementary DNA libraries according to the Illumina TruSeq RNA Sample Preparation v2 Guide for paired-end (2 \times 150) sequencing using the Illumina NextSeq 500 sequencing platform.

Prokaryotic metatranscriptome samples were collected during the R/V Ka'imikai-O-Kanaloa cruise KOK1606 (April–May 2016) in the North Pacific. Duplicate plankton samples of ~10 l of seawater were collected in the subtropical gyre (23° 48' N, 158° W). Plankton were sequentially filtered through a 3- μ m pre-filter followed by a 0.2- μ m polycarbonate filter using a peristaltic pump. Filters were flash frozen in liquid nitrogen and subsequently stored at -80°C until further processing. RNA was extracted as described above. Following DNase treatment, rRNAs were removed from the purified, total RNA using Illumina's Bacteria and Yeast Ribo-Zero rRNA Removal Kits. Depleted RNA was cleaned using the Zymo RNA Clean and Concentrator Kit. Purified, depleted RNA was then sheared to ~225-bp fragments and used to construct TruSeq cDNA libraries according to the Illumina TruSeq RNA Sample Preparation v2 Guide for paired-end (2 \times 150) sequencing using the Illumina NovaSeq 6000 sequencing platform.

Bioinformatics. Raw Illumina data were quality controlled with trimmomatic v0.36 (ref. ⁵⁸) using the parameters MAXINFO:135:0.5, LEADING:3, TRAILING:3, MINLEN:60 and AVGQUAL:20, and matching read pairs were merged using flash v1.2.11 (ref. ⁵⁹) with parameters -r 150 -f 250 -s 25. FASTQ files were converted to FASTA and translated with seqret and transeq vEMBOSS:6.6.0.0 (ref. ⁶⁰) using Standard Genetic Code. Potential coding frames with ≥ 40 uninterrupted amino acids were retained for further analysis.

Full-length, experimentally verified protein sequences (locus tags given in Supplementary Tables 4 and 10) from reference genomes were used as queries to identify putative orthologues in marine prokaryotic and eukaryotic genomes and transcriptome assemblies available through the Joint Genome Institute (JGI),

National Center for Biotechnology Information (NCBI) and the Marine Microbial Eukaryote Transcriptome Sequence Project (MMETSP)⁶¹ using BLASTp v2.2.31. Those sequences that came from JGI reference genomes (Supplementary Tables 4 and 10) were considered homologues if they were reciprocal best blast hits with the experimentally verified sequences that were used in the original queries. JGI and MMETSP sequences retrieved from the BLASTp search were clustered using usearch⁶² (typically with an identity of >80%) and aligned using MAFFT (version 7) with the E-INS-I algorithm⁶³. The alignment was trimmed using trimAl v1.2 using -gt .05 -resoverlap 0.5 -seqoverlap 50 options⁶⁴. The trimmed alignment file was converted to Phylip format, and the best-fit amino acid substitution matrix, among-site rate heterogeneity model and the observed amino acid frequency were determined using ProtTest 3 software⁶⁵. A maximum-likelihood phylogenetic reference tree was built using RAxML version 8 (ref. ⁶⁶), and only those sequences that clustered with experimentally verified enzymes were considered putative homologues.

To recruit environmental metatranscriptomic reads to the reference sequence alignments, an hmm profile was constructed from each reference alignment using hmmbuild, followed by transcript identification and alignment to the reference using hmmssearch (parameters: -T 40 -incT 40) and hmmlalign, respectively, with the HMMER package v3.1b2 (ref. ⁶⁷). NCBI taxonomy was assigned to each environmental sequence using pplacer v1.1.alpha19-0-g807f6f3 (ref. ⁶⁸) based on the read placement with the best maximum-likelihood score to the reference tree (parameters: --keep-at-most 1). Read counts for each edge were normalized by recovery of internal mRNA standards to estimate natural transcript abundance per litre of seawater⁵⁷. Statistical significance for diel periodicity of transcripts was determined using the Rhythmicity Analysis Incorporating Non-Parametric Methods (RAIN) package in R⁶⁹, and *P* values were corrected for false discovery rate using the Bonferroni correction method.

SAR11 isolation and growth. '*Candidatus* Pelagibacter sp. NP1' was isolated from a dilution to extinction high-throughput cultivation experiment as previously described⁷⁰. Briefly, bacteria from a depth of 40 m in the North Pacific (47° 49.839' N, 129° 44.990' W) were diluted to a final concentration of 1.67 cells ml⁻¹ in filter-sterilized seawater medium collected from the same location in July 2017. The seawater media were filtered through a 0.8- μ m pre-filter followed by a tangential flow filtration system (Millipore) equipped with a 30-kDa filter. This filtered seawater was then supplemented with 20 μ M DHPS in an attempt to select for SAR11. One millilitre of diluted cells was added to each well of a sterilized 96-well Teflon plate. Plates were incubated at in situ temperature (13 $^{\circ}\text{C}$). Cell densities were determined every 7 d for 3 weeks by staining with SYBR Green1 (Invitrogen) and enumeration using an EasyCyte Plus Flow Cytometer (Millipore). Bacteria in culture wells that were positive for growth were identified by 16S rRNA sequence analysis; the partial 16S sequence for strain NP1 (~99% identical to '*Candidatus* Pelagibacter ubique' strain HTCC1062) is deposited in NCBI's GenBank under accession number MH923014. Strain NP1 was subsequently transferred to larger culture volumes (up to 1 l). The cultures were then transferred into artificial marine seawater media (AMS1) prepared as previously described for '*Candidatus* P. ubique' strain HTCC1062 (ref. ⁴³) with some modifications; the media were prepared using the same base salts, macronutrients, trace metals and vitamins, but ammonium sulfate (NH₄)₂SO₄, myo-inositol and 4-aminobenzoic acid were not added. No organic buffers (HEPES or EDTA) were added, and the media were sparged with filtered CO₂ and with air to form a bicarbonate-based buffer as previously described⁴³. The media were then amended with equal molar amounts (25 μ M) of DMSP or methionine, DHPS or pyruvate, and glycine or taurine. Growth experiments were carried out in 50-ml volumes in acid-washed 250-ml polycarbonate bottles in biological triplicates with a starting concentration of 2.0 \times 10³ cells ml⁻¹. Analysis of variance and Tukey's honest significance tests were performed in R to identify significant differences between mean growth rates across treatments and final cell densities across treatments. Culture identity and purity were verified before and after all growth experiments and in each biological replicate by 16S rRNA sequence analysis.

Reporting Summary. Further information on research design is available in the Nature Research Reporting Summary linked to this article.

Data availability

KM1513 cruise information and associated data for the HOE Legacy II cruise can be found online at <http://hahana.soest.hawaii.edu/hoelegacy/hoelegacy.html>. Raw sequence data for the diel eukaryotic metatranscriptomes are available in the NCBI Sequence Read Archive under BioProject ID PRJNA492142. Raw sequence data for the prokaryotic metatranscriptomes are available under BioProject ID PRJNA492143. Metabolomics data are available in Metabolomics Workbench under project ID PR000797.

Code availability

The custom code used is available on GitHub at <https://github.com/IngallsLabUW> and <https://github.com/armbrustlab>.

Received: 26 September 2018; Accepted: 6 June 2019;
Published online: 22 July 2019

References

- Field, C. B. Primary production of the biosphere: integrating terrestrial and oceanic components. *Science* **281**, 237–240 (1998).
- Azam, F. & Malfatti, F. Microbial structuring of marine ecosystems. *Nat. Rev. Microbiol.* **5**, 782–791 (2007).
- Ksionzek, K. B. et al. Dissolved organic sulfur in the ocean: biogeochemistry of a petagram inventory. *Science* **354**, 456–459 (2016).
- Levine, N. M. Putting the spotlight on organic sulfur: diverse dissolved organic sulfur compounds play an active role in ocean biogeochemistry. *Science* **354**, 418–419 (2016).
- Tripp, H. J. et al. SAR11 marine bacteria require exogenous reduced sulphur for growth. *Nature* **452**, 741–744 (2008).
- Dupont, C. L. et al. Genomic insights to SAR86, an abundant and uncultivated marine bacterial lineage. *ISME J.* **6**, 1186–1199 (2012).
- Kiene, R. P., Linn, L. J., González, J., Moran, M. A. & Bruton, J. A. Dimethylsulfoniopropionate and methanethiol are important precursors of methionine and protein-sulfur in marine bacterioplankton. *Appl. Environ. Microbiol.* **65**, 4549–4558 (1999).
- Autry, A. R. & Fitzgerald, J. W. Sulfonate S: a major form of forest soil organic sulfur. *Biol. Fertil. Soils* **10**, 50–56 (1990).
- Cook, A. M., Denger, K. & Smits, T. H. M. Dissimilation of C3-sulfonates. *Arch. Microbiol.* **185**, 83–90 (2006).
- Cook, A. M. & Denger, K. Dissimilation of the C2 sulfonates. *Arch. Microbiol.* **179**, 1–6 (2002).
- Denger, K. et al. Sulphoglycolysis in *Escherichia coli* K-12 closes a gap in the biogeochemical sulphur cycle. *Nature* **507**, 114–117 (2014).
- Denger, K. & Cook, A. M. Racemase activity effected by two dehydrogenases in sulfolactate degradation by *Chromohalobacter salexigens*: purification of (S)-sulfolactate dehydrogenase. *Microbiology* **156**, 967–974 (2010).
- Mayer, J. et al. 2,3-Dihydroxypropane-1-sulfonate degraded by *Cupriavidus pinatubonensis* JMP134: purification of dihydroxypropanesulfonate 3-dehydrogenase. *Microbiology* **156**, 1556–1564 (2010).
- Warshan, D. et al. Feathermoss and epiphytic *Nostoc* cooperate differently: expanding the spectrum of plant–cyanobacteria symbiosis. *ISME J.* **11**, 2821–2833 (2017).
- Weinitschke, S., Sharma, P. I., Stingl, U., Cook, A. M. & Smits, T. H. M. Gene clusters involved in isethionate degradation by terrestrial and marine bacteria. *Appl. Environ. Microbiol.* **76**, 618–621 (2010).
- Denger, K. et al. Bifurcated degradative pathway of 3-sulfolactate in *Roseovarius nubinhibens* ISM via sulfoacetaldehyde acetyltransferase and (S)-cysteate sulfolylase. *J. Bacteriol.* **191**, 5648–5656 (2009).
- Denger, K., Smits, T. H. M. & Cook, A. M. L-Cysteate sulphylo-lyase, a widespread pyridoxal 5'-phosphate-coupled desulphonative enzyme purified from *Silicibacter pomeroyi* DSS-3^T. *Biochem. J.* **394**, 657–664 (2006).
- Landa, M., Burns, A. S., Roth, S. J. & Moran, M. A. Bacterial transcriptome remodeling during sequential co-culture with a marine dinoflagellate and diatom. *ISME J.* **11**, 2677–2690 (2017).
- Durham, B. P. et al. Cryptic carbon and sulfur cycling between surface ocean plankton. *Proc. Natl Acad. Sci. USA* **112**, 453–457 (2015).
- Durham, B. P. et al. Recognition cascade and metabolite transfer in a marine bacteria–phytoplankton model system. *Environ. Microbiol.* **19**, 3500–3513 (2017).
- Amin, S. A. et al. Interaction and signalling between a cosmopolitan phytoplankton and associated bacteria. *Nature* **522**, 98–101 (2015).
- Celik, E. et al. Metabolism of 2,3-dihydroxypropane-1-sulfonate by marine bacteria. *Org. Biomol. Chem.* **15**, 2919–2922 (2017).
- Jackson, A. E., Ayer, S. W. & Laycock, M. V. The effect of salinity on growth and amino acid composition in the marine diatom *Nitzschia pungens*. *Can. J. Bot.* **70**, 2198–2201 (1992).
- Boroujerdi, A. F. B. et al. Identification of isethionic acid and other small molecule metabolites of *Fragilariopsis cylindrus* with nuclear magnetic resonance. *Anal. Bioanal. Chem.* **404**, 777–784 (2012).
- Graham, D. E., Taylor, S. M., Wolf, R. Z. & Namboori, S. C. Convergent evolution of coenzyme M biosynthesis in the Methanosarcinales: cysteate synthase evolved from an ancestral threonine synthase. *Biochem. J.* **424**, 467–478 (2009).
- Götz, F. et al. Targeted metabolomics reveals proline as a major osmolyte in the chemolithoautotroph *Sulfurimonas denitrificans*. *MicrobiologyOpen* **7**, e00586 (2018).
- Ho, T. et al. The elemental composition of some marine phytoplankton. *J. Phycol.* **39**, 1145–1159 (2003).
- Hunter, J. E. et al. Lipidomics of *Thalassiosira pseudonana* under phosphorus stress reveal underlying phospholipid substitution dynamics and novel diglycosylceramide substitutes. *Appl. Environ. Microbiol.* **84**, e02034-17 (2018).
- Helgadóttir, S., Rosas-Sandoval, G., Söll, D. & Graham, D. E. Biosynthesis of phosphoserine in the Methanococcales. *J. Bacteriol.* **189**, 575–582 (2007).
- Tevatia, R. et al. The taurine biosynthetic pathway of microalgae. *Algal Res.* **9**, 21–26 (2015).
- Agnello, G., Chang, L. L., Lamb, C. M., Georgiou, G. & Stone, E. M. Discovery of a substrate selectivity motif in amino acid decarboxylases unveils a taurine biosynthesis pathway in prokaryotes. *ACS Chem. Biol.* **8**, 2264–2271 (2013).
- Krejci, Z., Hollemeyer, K., Smits, T. H. M. & Cook, A. M. Isethionate formation from taurine in *Chromohalobacter salexigens*: purification of sulfoacetaldehyde reductase. *Microbiology* **156**, 1547–1555 (2010).
- Felix, A.-K., Spittler, D., Klebensberger, J. & Schleheck, D. Entner–Doudoroff pathway for sulfoquinovose degradation in *Pseudomonas putida* SQ1. *Proc. Natl Acad. Sci. USA* **112**, E4298–E4305 (2015).
- Busby, W. F. & Benson, A. A. Sulfonic acid metabolism in the diatom *Navicula pelliculosa*. *Plant Cell Physiol.* **14**, 1123–1132 (1973).
- Busby, W. *Studies on the Identification and Metabolism of the Sulfonic Acids, Cysteinoic Acid and Sulfolpropanediol, in the Diatom Navicula pelliculosa, and their Distribution in the Major Algal Groups*. PhD dissertation, University of California San Diego (1966).
- Graupner, M., Xu, H. & White, R. H. Identification of an archaeal 2-hydroxy acid dehydrogenase catalyzing reactions involved in coenzyme biosynthesis in methanoarchaea. *J. Bacteriol.* **182**, 3688–3692 (2000).
- Kopriva, S. et al. Light regulation of assimilatory sulphate reduction in *Arabidopsis thaliana*. *Plant J.* **20**, 37–44 (1999).
- Wilson, S. T. et al. Coordinated regulation of growth, activity and transcription in natural populations of the unicellular nitrogen-fixing cyanobacterium *Crocospaera*. *Nat. Microbiol.* **2**, 17118 (2017).
- Bates, T. S. et al. The cycling of sulfur in surface seawater of the northeast Pacific. *J. Geophys. Res.* **99**, 7835–7843 (1994).
- Johnson, W. M., Kido Soule, M. C. & Kujawinski, E. B. Extraction efficiency and quantification of dissolved metabolites in targeted marine metabolomics. *Limnol. Oceanogr. Methods* **15**, 417–428 (2017).
- McCarren, J. et al. Microbial community transcriptomes reveal microbes and metabolic pathways associated with dissolved organic matter turnover in the sea. *Proc. Natl Acad. Sci. USA* **107**, 16420–16427 (2010).
- Fuhrman, J. A. & Hagstrom, A. in *Microbial Ecology of the Oceans* (ed. Kirchman, D. L.) 45–90 (John Wiley & Sons, 2008).
- Carini, P., Steindler, L., Beszteri, S. & Giovannoni, S. J. Nutrient requirements for growth of the extreme oligotroph ‘*Candidatus Pelagibacter ubique*’ HTCC1062 on a defined medium. *ISME J.* **7**, 592–602 (2013).
- Schwalbach, M. S., Tripp, H. J., Steindler, L., Smith, D. P. & Giovannoni, S. J. The presence of the glycolysis operon in SAR11 genomes is positively correlated with ocean productivity. *Environ. Microbiol.* **12**, 490–500 (2010).
- Tripp, H. J. et al. Unique glycine-activated riboswitch linked to glycine-serine auxotrophy in SAR11. *Environ. Microbiol.* **11**, 230–238 (2009).
- Reisch, C. R., Moran, M. A. & Whitman, W. B. Bacterial catabolism of dimethylsulfoniopropionate (DMSP). *Front. Microbiol.* **2**, 172 (2011).
- Sun, J. et al. The abundant marine bacterium *Pelagibacter* simultaneously catabolizes dimethylsulfoniopropionate to the gases dimethyl sulfide and methanethiol. *Nat. Microbiol.* **1**, 16065 (2016).
- Seymour, J. R., Amin, S. A., Raina, J.-B. & Stocker, R. Zooming in on the phycosphere: the ecological interface for phytoplankton–bacteria relationships. *Nat. Microbiol.* **2**, 17065 (2017).
- Luo, H., Csuros, M., Hughes, A. L. & Moran, M. A. Evolution of divergent life history strategies in marine alphaproteobacteria. *mBio* **4**, e00373-13 (2013).
- Giovannoni, S. J. SAR11 bacteria: the most abundant plankton in the oceans. *Ann. Rev. Mar. Sci.* **9**, 231–255 (2017).
- Boysen, A. K., Heal, K. R., Carlson, L. T. & Ingalls, A. E. Best-matched internal standard normalization in liquid chromatography–mass spectrometry metabolomics applied to environmental samples. *Anal. Chem.* **90**, 1363–1369 (2018).
- MacLean, B. et al. Skyline: an open source document editor for creating and analyzing targeted proteomics experiments. *Bioinformatics* **26**, 966–968 (2010).
- Smith, C. A., Want, E. J., O’Maille, G., Abagyan, R. & Siuzdak, G. XCMS: processing mass spectrometry data for metabolite profiling using nonlinear peak alignment, matching, and identification. *Anal. Chem.* **78**, 779–787 (2006).
- Boiteau, R. M. & Repeta, D. J. An extended siderophore suite from *Synechococcus* sp. PCC 7002 revealed by LC-ICPMS-ESIMS. *Metallomics* **7**, 877–884 (2015).
- Tsugawa, H. et al. MS-DIAL: data-independent MS/MS deconvolution for comprehensive metabolome analysis. *Nat. Methods* **12**, 523–526 (2015).
- Patiny, L. & Borel, A. ChemCalc: a building block for tomorrow’s chemical infrastructure. *J. Chem. Inf. Model.* **53**, 1223–1228 (2013).
- Satinsky, B. M., Gifford, S. M., Crump, B. C. & Moran, M. A. Use of internal standards for quantitative metatranscriptome and metagenome analysis. *Methods Enzymol.* **531**, 237–250 (2013).
- Bolger, A. M., Lohse, M. & Usadel, B. Trimmomatic: a flexible trimmer for Illumina sequence data. *Bioinformatics* **30**, 2114–2120 (2014).

59. Magoč, T., Magoč, M. & Salzberg, S. L. FLASH: fast length adjustment of short reads to improve genome assemblies. *Bioinformatics* **27**, 2957–2963 (2011).
60. Rice, P., Longden, I. & Bleasby, A. EMBOSS: the European Molecular Biology Open Software Suite. *Trends Genet.* **16**, 276–277 (2000).
61. Keeling, P. J. et al. The Marine Microbial Eukaryote Transcriptome Sequencing Project (MMETSP): illuminating the functional diversity of eukaryotic life in the oceans through transcriptome sequencing. *PLoS Biol.* **12**, e1001889 (2014).
62. Edgar, R. C. Search and clustering orders of magnitude faster than BLAST. *Bioinformatics* **26**, 2460–2461 (2010).
63. Katoh, K. & Standley, D. M. MAFFT multiple sequence alignment software version 7: improvements in performance and usability. *Mol. Biol. Evol.* **30**, 772–780 (2013).
64. Capella-Gutiérrez, S., Silla-Martínez, J. M. & Gabaldón, T. trimAl: a tool for automated alignment trimming in large-scale phylogenetic analyses. *Bioinformatics* **25**, 1972–1973 (2009).
65. Darriba, D., Taboada, G. L., Doallo, R. & Posada, D. ProtTest 3: fast selection of best-fit models of protein evolution. *Bioinformatics* **27**, 1164–1165 (2011).
66. Stamatakis, A., Hoover, P. & Rougemont, J. A rapid bootstrap algorithm for the RAxML web servers. *Syst. Biol.* **57**, 758–771 (2008).
67. Eddy, S. R. Accelerated profile HMM searches. *PLoS Comput. Biol.* **7**, e1002195 (2011).
68. Matsen, F. A., Kodner, R. B. & Armbrust, V. pplacer: linear time maximum-likelihood and Bayesian phylogenetic placement of sequences onto a fixed reference tree. *BMC Bioinformatics* **11**, 538 (2010).
69. Thaben, P. F. & Westermark, P. O. Detecting rhythms in time series with RAIN. *J. Biol. Rhythms* **29**, 391–400 (2014).
70. Marshall, K. T. & Morris, R. M. Isolation of an aerobic sulfur oxidizer from the SUP05/Arctic96BD-19 clade. *ISME J.* **7**, 452–455 (2013).

Acknowledgements

The data sets presented here resulted from the contributions of many scientists. We acknowledge laboratory assistance from M. Schatz, R. Boccamazzo, G. Workman,

N. Kellogg, A. Weid and R. Lionheart. Cultures were kindly provided by R. Cattolico, S. Chisholm, A. Coe, C. Deodato, M. Moran and M. Saito. Assistance with untargeted metabolomics data analysis was generously provided by R. Boiteau. We also thank J. Becker, J. Collins, F. Ribalet, J. Saunders, M. Moran and S. Amin for helpful discussion and feedback. We thank the crew members of the R/V Kilo Moana and S. Wilson for cruise leadership (KM1513), the crew members of the R/V Ka'imikai-O-Kanaloa (KOK1606) and the operational staff of the Simons Collaboration on Ocean Processes and Ecology (SCOPE). This work was supported by grants from the National Science Foundation (Award ID OCE PRF-1521564 to B.P.D. and Award ID OCE-1558483 to R.M.M. and A.E.I.), the Simons Foundation (SCOPE Award ID 329108 to E.V.A. and A.E.I., SF Award ID 385428 to A.E.I. and SF Award ID 426570 to E.V.A.) and the Gordon and Betty Moore Foundation (GBMF3776 to E.V.A.).

Author contributions

B.P.D., R.M.M., A.E.I. and E.V.A. designed the study. B.P.D., A.K.B., L.T.C. and K.R.H. generated and analysed the metabolomics data. B.P.D., R.D.G., R.L.M. and S.N.C. generated and analysed the metatranscriptomics data. K.R.C. and R.M.M. performed the SAR11 culture experiments. B.P.D., R.M.M., A.E.I. and E.V.A. wrote the manuscript with contributions from all authors.

Competing interests

The authors declare no competing interests.

Additional information

Supplementary information is available for this paper at <https://doi.org/10.1038/s41564-019-0507-5>.

Reprints and permissions information is available at www.nature.com/reprints.

Correspondence and requests for materials should be addressed to B.P.D.

Publisher's note: Springer Nature remains neutral with regard to jurisdictional claims in published maps and institutional affiliations.

© The Author(s), under exclusive licence to Springer Nature Limited 2019

Reporting Summary

Nature Research wishes to improve the reproducibility of the work that we publish. This form provides structure for consistency and transparency in reporting. For further information on Nature Research policies, see [Authors & Referees](#) and the [Editorial Policy Checklist](#).

Statistical parameters

When statistical analyses are reported, confirm that the following items are present in the relevant location (e.g. figure legend, table legend, main text, or Methods section).

n/a | Confirmed

- The exact sample size (n) for each experimental group/condition, given as a discrete number and unit of measurement
- An indication of whether measurements were taken from distinct samples or whether the same sample was measured repeatedly
- The statistical test(s) used AND whether they are one- or two-sided
Only common tests should be described solely by name; describe more complex techniques in the Methods section.
- A description of all covariates tested
- A description of any assumptions or corrections, such as tests of normality and adjustment for multiple comparisons
- A full description of the statistics including central tendency (e.g. means) or other basic estimates (e.g. regression coefficient) AND variation (e.g. standard deviation) or associated estimates of uncertainty (e.g. confidence intervals)
- For null hypothesis testing, the test statistic (e.g. F , t , r) with confidence intervals, effect sizes, degrees of freedom and P value noted
Give P values as exact values whenever suitable.
- For Bayesian analysis, information on the choice of priors and Markov chain Monte Carlo settings
- For hierarchical and complex designs, identification of the appropriate level for tests and full reporting of outcomes
- Estimates of effect sizes (e.g. Cohen's d , Pearson's r), indicating how they were calculated
- Clearly defined error bars
State explicitly what error bars represent (e.g. SD, SE, CI)

Our web collection on [statistics for biologists](#) may be useful.

Software and code

Policy information about [availability of computer code](#)

Data collection

Metabolomics data was collected using instrument software on Waters Xevo TQ-S triple quadrupole and Thermo QExactive HF mass spectrometers.

Data analysis

Software and code used for metabolite and transcript analyses are described and cited within the methods; this information is summarized below:

Analysis of targeted metabolomics data was performed according to the published protocols found in Boysen and Heal et al., 2018. This code is available on GitHub at <https://github.com/IngallsLabUW>. Peak integrations were performed using Skyline v4.1 (MacLean et al., 2010).

Untargeted metabolomics data was processed using XCMS v3.7 (Smith et al., 2006; Tautenhahn et al., 2008; Benton et al., 2010). Sulfur-isotope analysis of untargeted metabolomics data was performed using a search algorithm published in Boiteau et al., 2015, 2016. This algorithm was previously developed for Fe identification, and it was modified for S identification. MS2 fragments for cysteinolic acid were extracted using MS-DIAL v3.08 (Tugawa et al., 2015) and Xcaliber v4.1 (Thermo Scientific).

Tools used in gene homolog identification and reference tree construction are publicly available:

search v10.0.240_i86linux32 (sequence clustering; found in Edgar, 2010)
MAFFT v7 (sequence alignment; found in Katoh and Standley, 2013)
trimAl v1.2 (alignment trimming; found in Capella-Gutierrez et al., 2009)

ProtTest 3 (amino acid modeling; found in Darriba et al., 2011 and Guindon and Gascuel, 2003)
 RAxML v8 (reference tree construction; found in Stamatakis et al., 2008 and Stamatakis, 2014)

Tools used in the analysis of transcriptome data are listed below, with any modifications and/or parameters described in the methods:
 trimmomatic v0.36 (quality control; found in Bolger et al., 2014)
 flash v1.2.11 (merging of paired reads; found in Magoc et al., 2011)
 seqret and transeq vEMBOSS:6.6.0.0 (format conversion and translation, found in Rice et al., 2000)
 HMMer package v3.1b2 (hmm profile and read alignment; found in Eddy, 2011)
 pplacer v1.1.alpha19-0-g807f6f3 (taxonomy assignment; found in Matsen et al., 2010)

Statistical analysis of transcripts and metabolites for diel periodicity was performed using the Rhythmicity Analysis Incorporating Non-parametric Methods (RAIN) package in R (Thaben and Westermark, 2014).

Code for metatranscriptome analyses is available on GitHub at <https://github.com/armbrustlab>.

For manuscripts utilizing custom algorithms or software that are central to the research but not yet described in published literature, software must be made available to editors/reviewers upon request. We strongly encourage code deposition in a community repository (e.g. GitHub). See the Nature Research [guidelines for submitting code & software](#) for further information.

Data

Policy information about [availability of data](#)

All manuscripts must include a [data availability statement](#). This statement should provide the following information, where applicable:

- Accession codes, unique identifiers, or web links for publicly available datasets
- A list of figures that have associated raw data
- A description of any restrictions on data availability

KM1513 cruise information and associated data for the HOE Legacy II cruise can be found online at <http://hahana.soest.hawaii.edu/hoelegacy/hoelegacy.html>. Raw sequence data for the diel eukaryotic metatranscriptomes are available in the NCBI Sequence Read Archive under BioProject ID PRJNA492142. Raw sequence data for the prokaryotic metatranscriptomes are available under BioProject ID PRJNA492143. Metabolomics data are available in Metabolomics Workbench under Project ID PR000795.

The following figures have associated raw data:

Figure 2
 Figure 3
 Supplementary Figure 2
 Supplementary Figure 3
 Supplementary Figure 4

There are no restrictions on data availability.

Field-specific reporting

Please select the best fit for your research. If you are not sure, read the appropriate sections before making your selection.

Life sciences Behavioural & social sciences Ecological, evolutionary & environmental sciences

For a reference copy of the document with all sections, see [nature.com/authors/policies/ReportingSummary-flat.pdf](https://www.nature.com/authors/policies/ReportingSummary-flat.pdf)

Ecological, evolutionary & environmental sciences study design

All studies must disclose on these points even when the disclosure is negative.

Study description

LABORATORY STUDIES:

To identify the marine microbial taxa that produce sulfonates, a targeted liquid chromatography-mass spectrometry-based metabolomics method was used to screen the intracellular metabolite pools of 36 plankton taxa. All cultures were grown in artificial, defined media and collected in biological replicates (n=2 or 3) during late exponential growth phase.

FIELD STUDIES:

To measure the expression patterns for sulfonate metabolism genes and sulfonate abundances in North Pacific plankton populations, metatranscriptomes and metabolomes were collected, respectively, in biological replicates (n=2 or 3).

Research sample

LABORATORY STUDIES:

Cells were collected for autotrophic eukaryotic stramenopiles (e.g. diatoms), alveolates (e.g. dinoflagellates), haptophytes (e.g. coccolithophores), and green algae (e.g. prasinophytes), and autotrophic and heterotrophic bacteria (e.g. cyanobacteria, alpha-, gamma-, and beta-proteobacteria, flavobacteria).

These taxa were chosen because they represent a broad range of important marine plankton groups, and the specific species were chosen based on their axenic status (purity) and their ability to grow in artificial, defined media.

FIELD STUDIES:

Natural plankton were collected from surface seawater by filtration.

Sampling strategy	Cells were collected onto 0.2-micron filters and flash frozen in liquid nitrogen. Biological replicates were collected for all cultures and field samples (n=2 or 3). This replication is typical for current metabolomic analyses (Boysen and Heal et al., 2018) and metatranscriptomic analyses (Satinsky et al., 2013).
Data collection	<p>Biological and physiological measurements (growth conditions, cell count, growth rate, etc) were collected by Durham. These measurements were documented in a laboratory notebook and transcribed later to electronic csv files.</p> <p>Metabolomics data was generated by Carlson at UW (in the Ingalls lab) using Waters Xevo TQ-S triple quadrupole and Thermo QExactive HF mass spectrometers. Data is stored locally in the Ingalls lab.</p> <p>Metatranscriptomics data was generated at the UW Northwest Genomics Center and stored locally by Groussaman (in the Armbrust lab).</p>
Timing and spatial scale	<p>LABORATORY STUDIES: Cultures were collected and run on the mass spectrometer during April 2016 - December 2017. Phytoplankton cultures often take weeks to acclimate, so cultures were grown in batches and analyzed as they were collected.</p> <p>FIELD STUDIES: Field samples for the diel study were collected over four days (July 26 - 30, 2015) and analyzed within a year of collection.</p>
Data exclusions	No data were excluded.
Reproducibility	<p>LABORATORY STUDIES: In some cases, cultures were grown multiple times and analyzed (several cyanobacteria and diatoms). Our results were always consistent across samples.</p> <p>FIELD STUDIES: In the diel study, we collected data over 4 days. The 24-hour day-night patterns were consistent over the four days.</p>
Randomization	<p>LABORATORY STUDIES: Cultures were extracted for metabolites in batches as they were collected (not randomized). This is due to the length of time required to culture 36 organisms. However, samples within a batch were run on the mass spectrometer in randomized order. Internal standards were added to all samples (both extraction and instrument injection standards) to allow cross comparison between batches and machine runs.</p> <p>FIELD STUDIES: Metabolomic samples were extracted in batches and run on the mass spectrometer in randomized order. Internal standards were added to all samples (both extraction and instrument injection standards) to allow cross comparison between batches and machine runs.</p> <p>Metatranscriptomic samples were extracted and sequenced in randomized order. Internal standards (added at extraction) were used for cross comparison across all samples.</p>
Blinding	<p>Blinding was not used for these samples. Because samples for metabolomics require dilutions and internal standard additions prior to running on the instrument, the type of sample is taken into account before extraction and analysis. Similarly, transcriptomics samples require addition of internal standards and specific processing steps that require information on the type of sample before extraction and sequencing.</p>
Did the study involve field work?	<input checked="" type="checkbox"/> Yes <input type="checkbox"/> No

Field work, collection and transport

Field conditions	Plankton samples for metatranscriptomics and particulate metabolomics were collected in the North Pacific Subtropical Gyre during sea-going field expeditions in spring/summer.
Location	<p>For eukaryotic metatranscriptomics and particulate metabolomics sampling, a Lagrangian approach was used to sample from the same water parcel over the four days by following free-drifting drogues centered at a depth of 15 m (approximately 24.4 N 156.5 W, near Station ALOHA). All samples were collected from 15 m depth within the surface mixed layer.</p> <p>Prokaryotic metatranscriptomics samples were collected in the same region (23.48 N, 158 W) in April-May 2016, also at 15 m depth.</p>
Access and import/export	Environmental samples were collected during two cruises (KM1513 and KOK1606) in compliance with University of Hawaii, University of Washington, and UNOLS practices.
Disturbance	NA

Reporting for specific materials, systems and methods

Materials & experimental systems

n/a	Involvement in the study
<input type="checkbox"/>	<input checked="" type="checkbox"/> Unique biological materials
<input checked="" type="checkbox"/>	<input type="checkbox"/> Antibodies
<input checked="" type="checkbox"/>	<input type="checkbox"/> Eukaryotic cell lines
<input checked="" type="checkbox"/>	<input type="checkbox"/> Palaeontology
<input checked="" type="checkbox"/>	<input type="checkbox"/> Animals and other organisms
<input checked="" type="checkbox"/>	<input type="checkbox"/> Human research participants

Methods

n/a	Involvement in the study
<input checked="" type="checkbox"/>	<input type="checkbox"/> ChIP-seq
<input checked="" type="checkbox"/>	<input type="checkbox"/> Flow cytometry
<input checked="" type="checkbox"/>	<input type="checkbox"/> MRI-based neuroimaging

Unique biological materials

Policy information about [availability of materials](#)

Obtaining unique materials

We isolated an open-ocean bacterial strain (Ca. Pelagibacter ubique strain NP1) that belongs to the SAR11 clade. Members of this bacterial group are not routinely stored in culture collections, so the strain will be made available upon request.